Theoretical and Applied Climatology
https://doi.org/10.1007/s00704-018-2434-4

ORIGINAL PAPER

Return period curves for extreme 5-min rainfall amounts at the Barcelona urban network

X. Lana[1] · M. C. Casas-Castillo[1] · C. Serra[1] · R. Rodríguez-Solà[1] · A. Redaño[2] · A. Burgueño[2] · M. D. Martínez[1]

Received: 21 June 2017 / Accepted: 20 February 2018

Abstract
Heavy rainfall episodes are relatively common in the conurbation of Barcelona and neighbouring cities (NE Spain), usually due to storms generated by convective phenomena in summer and eastern and south-eastern advections in autumn. Prevention of local flood episodes and right design of urban drainage have to take into account the rainfall intensity spread instead of a simple evaluation of daily rainfall amounts. The database comes from 5-min rain amounts recorded by tipping buckets in the Barcelona urban network along the years 1994–2009. From these data, extreme 5-min rain amounts are selected applying the peaks-over-threshold method for thresholds derived from both 95% percentile and the mean excess plot. The return period curves are derived from their statistical distribution for every gauge, describing with detail expected extreme 5-min rain amounts across the urban network. These curves are compared with those derived from annual extreme time series. In this way, areas in Barcelona submitted to different levels of flood risk from the point of view of rainfall intensity are detected. Additionally, global time trends on extreme 5-min rain amounts are quantified for the whole network and found as not statistically significant.

Keywords Extreme 5-min rain amounts · Peaks-over-threshold · Mean excess plot · Annual extreme time series · Return periods · GP · GLO and GEV distributions · Significant time trends · Barcelona urban network

1 Introduction

The rainfall intensity in the Barcelona urban area has been analysed from different points of view and at different time scales along previous years, basically with two main objectives. On one hand, to achieve a better knowledge of statistical parameters characterising the different rainfall episodes together with synoptic and mesoscale conditions taking part in their generation; on the other hand, to get an analysis of extreme rainfall episodes, at daily scale and at short time intervals of a few minutes. It has to be taken into account that short but intense episodes may cause floods. Previous analyses covering some of these main objectives include the rainfall rates at local scale (Lorente and Redaño 1990), extreme rainfall events (Casas et al. 2004, 2010), the daily pluviometric regime at Fabra Observatory (Barcelona) (Burgueño et al. 2004; Lana et al. 2005), spatial and temporal characteristics of the rainfall rate in the Barcelona urban network (Rodríguez et al. 2013a,b), the intensity-duration-frequency curves (Rodríguez-Solà et al. 2016) and the statistical distribution of 5-min rain amounts for the Barcelona urban area (Lana et al. 2017).

In the present paper, two specific goals concerning extreme rainfall intensity are developed. First, peaks-over-threshold (POT) for extreme 5-min rain amounts are obtained for the set of gauges of the urban network of Barcelona. This POT approach has been usually applied to obtain extreme series of daily rainfall amounts and daily temperatures (i.e., Beguería et al. 2009; Kysely et al. 2010; Acero et al. 2011; Villarini et al. 2011; Anagnostopoulou and Tolika 2012). In here, these POT have been derived through two methodologies: 95% percentile and mean excess plot (MEP). Similar procedures were applied before to analyse the extreme duration of dry spells from partial duration series (Vicente-Serrano and Beguería-Portugués 2003; Beguería-Portugués 2005; Lana et al. 2006). Then, return period curves for extreme 5-min rain amounts are derived from their statistical distribution for every

✉ X. Lana
francisco.javier.lana@upc.edu

[1] Departament de Física, Universitat Politècnica de Catalunya, Barcelona, Spain

[2] Departament de Física Aplicada – Meteorologia, Universitat de Barcelona, Barcelona, Spain

gauge. Global time trends on extreme 5-min rain amounts, together with their statistical significance, are quantified for the whole set of gauges. Similar time trend quantifications are due to Acero et al. (2011) and Beguería et al. (2011), who studied extreme daily rainfall over the whole Iberian Peninsula and north-east Spain, respectively, or also to Chen and Chu (2014), who studied time trends of annual maximum daily precipitation in the Hawaiian Islands.

The contents of the paper are organised as follows. "Section 2" ("Database") briefly describes the characteristics of the urban network, as well as its spatial distribution throughout the city of Barcelona. "Section 3" ("Methodology") explains the 95% percentile and MEP methodologies applied to select extreme 5-min rain amounts. The statistical functions fitting better empiric distributions of extremes are chosen taking advantage of L-moments estimation, through L-skewness-kurtosis diagrams (Hosking et al. 1985; Hosking and Wallis 1997). "Section 4" ("Results") presents the characteristics of the return period curves, comparing results derived from annual extreme series (AES), 95% percentile, MEP and the evaluation of global linear time trends affecting extreme 5-min rain amounts, with their statistical significance. "Section 5" ("Conclusions") summarises the outstanding results, highlighting the areas of Barcelona City submitted to the expected highest extreme rain intensities.

2 Database

Since 1994, a dense network of 23 high-resolution tipping bucket rain rate gauges covers the urban area of Barcelona (approximately 100 km^2) (Fig. 1 and Table1). This rain gauge network has been run by CLABSA, a company that controlled the sewer systems of the city. Every gauge has a collector surface of 400 cm^2, with an amount resolution of 0.1 mm. The integration time applied to the rain rates measured is 1 min. The resulting intensities calculated for durations shorter than 1 h could have been affected by an error below 10%, whereas for durations longer than 2 h the error determining the intensity is generally smaller than 5% (Rodríguez et al. 2013a). The 5-min rain amounts are generated from a sample of 188 rainfall episodes recorded at the set of rain rate gauges since 1994 up to 2009, with wide ranges of lengths and rainfall amounts.

Along this period, there were some anomalous maintenance periods of the rain gauges that impeded the right rainfall measure. Bearing in mind that 6 out of the 23 gauges (gauge numbers 3, 4, 12, 13, 21 and 23) have not been operative for some years, the return period curves have been obtained for the remaining 17 gauges. Nevertheless, the best statistical distribution models and linear time trends on extreme 5-min rain amounts are tested for all the 23 gauges. For the 17 gauges selected and the 188 rainfall episodes analysed, the percentage of missed 5-min rain amounts is kept below 3%. The homogeneity of the rainfall time series has been verified by the application of Wald-Wolfowitz run test of randomness (Alhakim and Hooper 2008) and the Mann-Kendall trend test (Sneyers 1990). The resulting total number of 5-min rain amounts for the 188 episodes ranges from 3520 (gauge 17) to 4260 (gauge 1).

Prior to the application of the 95% percentile and MEP to obtain POT series of extreme 5-min amounts, it has to be remembered that time series of 5-min amounts follow the Weibull distribution, with different location, shape and scale parameters for every rain rate gauge (Lana et al. 2017). It is also relevant to note that the highest selected extreme 5-min rain amounts within the whole urban area range from 10 to 20 mm/5 min. In consequence, extreme 5-min amounts above these outstanding rainfall intensities are to be expected for long return periods. The possible resulting floods and urban drainage problems from these heavy intensities could be notable and serious, affecting the urban area of Barcelona.

3 Methodology

The procedure to obtain time series of extreme values with a certain degree of reliability sometimes is not straightforward nor efficient. For instance, when climatic or meteorological phenomena are analysed at annual scale, AES, made from the selection of the maximum annual values, is not so advisable. Even having recorded several values close to the annual maximum, just the maximum value would be added to the time series of annual extremes. In this way, empirical frequencies of extreme values, leading to statistical distribution functions and return period curves, could not be correctly quantified, especially for short recording periods. An alternative to solve this sampling shortcoming is the POT method. This consists of, first, rearranging in increasing order all the data series and, second, deciding which is the best threshold to define the optimum set of empirical extremes. This threshold could be obtained as the 95% percentile for every empiric distribution or applying the MEP as proposed by Vicente-Serrano and Beguería-Portugués (2003) and Beguería-Portugués (2005).

The first way is straightforward to apply. For every network gauge, after disposing the data in an increasing order, only those above the 95% percentile are considered as extreme values. The second way (MEP) consists of plotting the mean excess over a threshold against the threshold itself. It is expected that the MEP depicts a linear evolution up to the optimum truncation threshold. Then, extreme values are defined as those above this truncation level. Studies on extreme dry spell lengths (Lana et al. 2006) suggest that optimum thresholds used to be close to 95% percentile. Notwithstanding, from a pure empirical point of view, results obtained for the analysed rainfall intensity will show sometimes discrepancies when thresholds are derived from 95% percentile or from MEP.

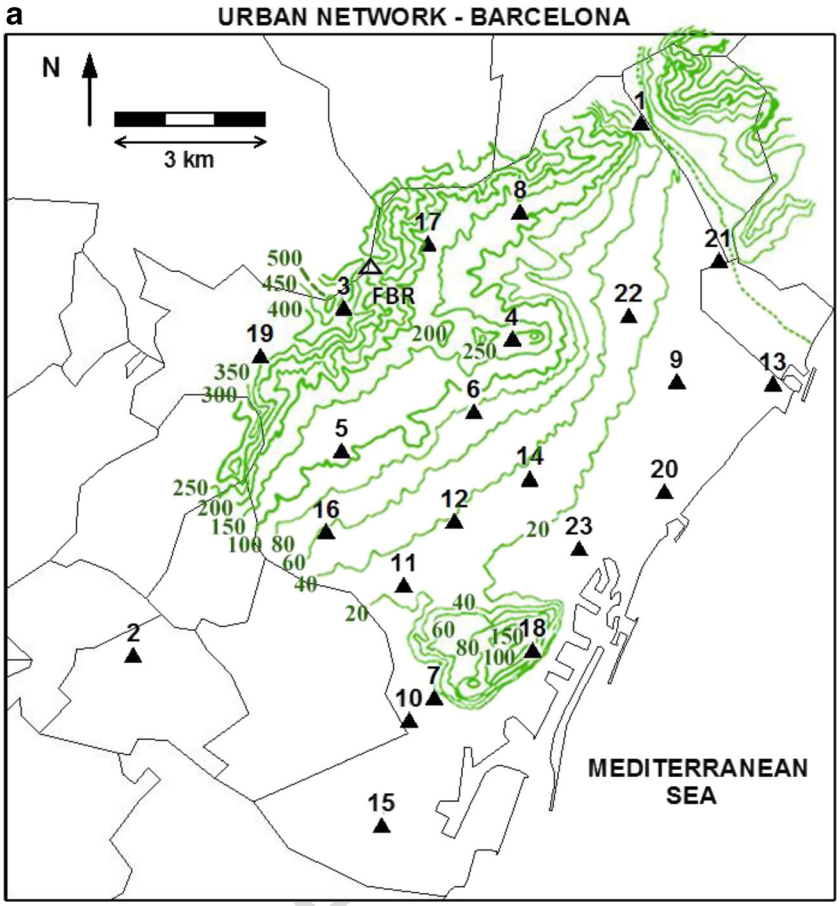

Fig. 1 **a** Urban network of 23 tipping bucket rain rate gauges in Barcelona (solid triangles). Topographic contour lines for the urban area are also included with altitudes above sea level ranging from 20 to 500 m. **b** Examples of autocorrelations for POT series, derived from 95% percentile, declustered 95% percentile and MEP criteria. Solid lines correspond to random series autocorrelation

In comparison with the AES, the POT strategy is a better solution for the analysis of the extreme 5-min rain by several reasons. Incomplete samples of extreme 5-min amounts would result with AES. Quite similarly, extreme 5-min amounts would then be discarded and the selected sample would be excessively short (a length equal to the number of recording years) for a confident quantification of statistics and return period curves. Conversely, POT are not made of annual extremes. The number of extreme 5-min amounts is expected to be large enough to permit a detailed search of the optimum threshold either 95% percentile or based on the MEP.

A relevant question is the independence of the POT samples, a necessary requirement for a right statistical modelling. The independence is required to be checked, given that the selected extremes may be consecutive in time. Then, Kendall's tau test was applied to every POT series to check the independence between the ordered samples (Kendall and Stuart 1967; Ferguson et al. 2000; Claps and Laio 2003). A detailed description of this procedure can be found in Appendix. The resulting τ parameter for every POT series is kept below the one-sided 95% test. Consequently, the independence of the ordered values is assumed. As a second test, the autocorrelation of every POT series has been computed for different lags. Only for lag equal to 1, moderate signs, $\phi(1) < 0.45$, of autocorrelation are found. It is worth mentioning that $\phi(1)$ obtained from MEP series are smaller than those derived from 95% percentile series. In consequence, the dependence of selected extremes is reduced when MEP option is considered. Two examples corresponding to gauges 1 and 6 are shown in Fig. 1b, where autocorrelations for 95% percentile and MEP criteria are compared with autocorrelation corresponding to random noise. In short, although some 5-min peaks may pertain to the same rainfall episode, this fact contributing to some correlation, the independence of POT series would be acceptable, especially when the MEP criterion is considered. As a third check, every one of the extreme series derived by considering a 95% threshold has been declustered by removing extremes below the highest extreme in the same episode. In this way, the hypothesis of independence is satisfied. An example of the declustered series autocorrelation is included in Fig. 1b. The procedure of declustering has not been applied to MEP series, given that the remaining number of extremes would be many times excessively short to a right determination of autocorrelation, statistical properties and return periods.

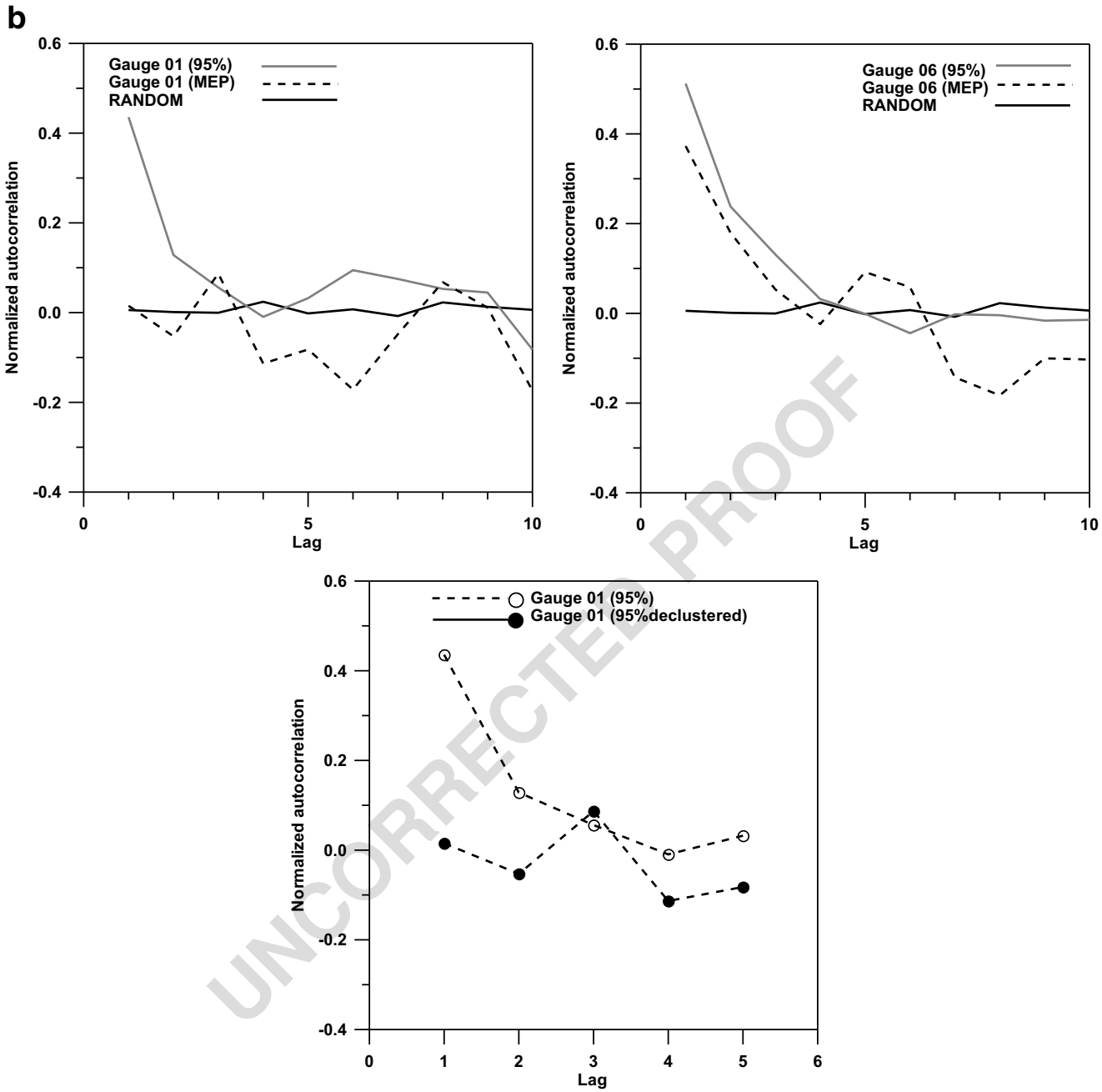

Fig. 1 (continued)

After obtaining the optimum set of values, the best statistical distribution can be determined by L-moments (Hosking et al. 1985; Hosking and Wallis 1997). Comparisons between empirical and several theoretical L-skewness-kurtosis curves permit deciding which is the best theoretical statistical distribution of extreme 5-min amounts. The best models at the present analysis are the generalised Pareto, GP, with probability density function

$$f(x) = \alpha^{-1} e^{-(1-k)y} \tag{1a}$$

$$y = -k^{-1} \log\left\{1 - \frac{k(x-\delta)}{\alpha}\right\}; k \neq 0 \tag{1b}$$

$$y = \frac{x-\delta}{\alpha}; k = 0. \tag{1c}$$

with x corresponding in this case to 5-min amounts; and α, k and δ, the scale, shape and location parameters. According to Coles (2001), the scale parameter α controls the spread of the observed distribution, in such a way that $F(x;\alpha,\kappa,\delta) = F\left(\frac{x}{\alpha};1,\kappa,\delta\right)$, F being the cumulative distribution of $f(x)$. Then, for larger (smaller) α, the observed distribution will be more spread out (concentrated). The location parameter δ controls the position of the distribution function along the horizontal axis, being

Q4 **Table 1** Altitude above sea level, *Z*, and UTM coordinates for the 23 gauges of the urban network

Gauge	*Z* (m)	*X* (UTM)	*Y* (UTM)
1	18	432572	4590189
2	15	422530	4579549
3	450	426690	4586494
4	162	430034	4585878
5	120	426648	4583627
6	86	429270	4584410
7	9	428485	4578698
8	148	430181	4588414
9	7	433279	4585023
10	4	427987	4578247
11	27	427879	4580946
12	37	428911	4582279
13	5	435184	4584975
14	32	430373	4583077
15	3	427443	4576149
16	67	426341	4582030
17	206	428357	4587775
18	146	430431	4579649
19	293	425042	4585529
20	3	433035	4582822
21	14	434117	4587439
22	26	432334	4586332
23	8	431351	4581678

UTM Universal Transverse Mercator

$F(x;\alpha,\kappa,\delta)=F(x-\delta;\alpha,\kappa,0)$. And, the shape parameter κ affects the shape of the distribution, rather than simply stretching/shrinking it (as the scale parameter does) or shifting it (as the location parameter does).

If δ is unknown, these parameters are given as

$$\alpha=(1+k)(2+k)\lambda_2 \quad (2a)$$

$$k=(1-3\tau_3)/(1+\tau_3) \quad (2b)$$

$$\delta=\lambda_1-(2+k)\lambda_2 \quad (2c)$$

λ_i ($i=1, 2, 3, 4$) are the first four L-moments; and $\tau_3=\lambda_3/\lambda_2$ and $\tau_4=\lambda_4/\lambda_2$, the L-skewness and L-kurtosis moments (Hosking and Wallis 1997). Scale, shape and location parameters permit defining the range of validity of argument x, given by $\{\delta\le x\le\delta+\alpha/\kappa\}$ if $\kappa>0$ and by $\{\delta\le x\le\infty\}$ if $\kappa\le 0$.

In a few cases, the generalised logistic GLO distribution

$$f(x)=\alpha^{-1}e^{-(1-k)y}/(1+e^{-y})^2 \quad (3a)$$

is a better option with

$$y=-k^{-1}\log\left\{1-\frac{k(x-\delta)}{\alpha}\right\};k\neq 0 \quad (3b)$$

$$y=\frac{x-\delta}{\alpha};k=0 \quad (3c)$$

where scale, α, shape, k, and location, δ, parameters are given as

$$\alpha=\lambda_2\sin(\pi k)/(\pi k) \quad (4a)$$

$$k=-\tau_3 \quad (4b)$$

$$\delta=\lambda_1-\alpha\left(\frac{1}{k}-\pi/\sin(\pi k)\right) \quad (4c)$$

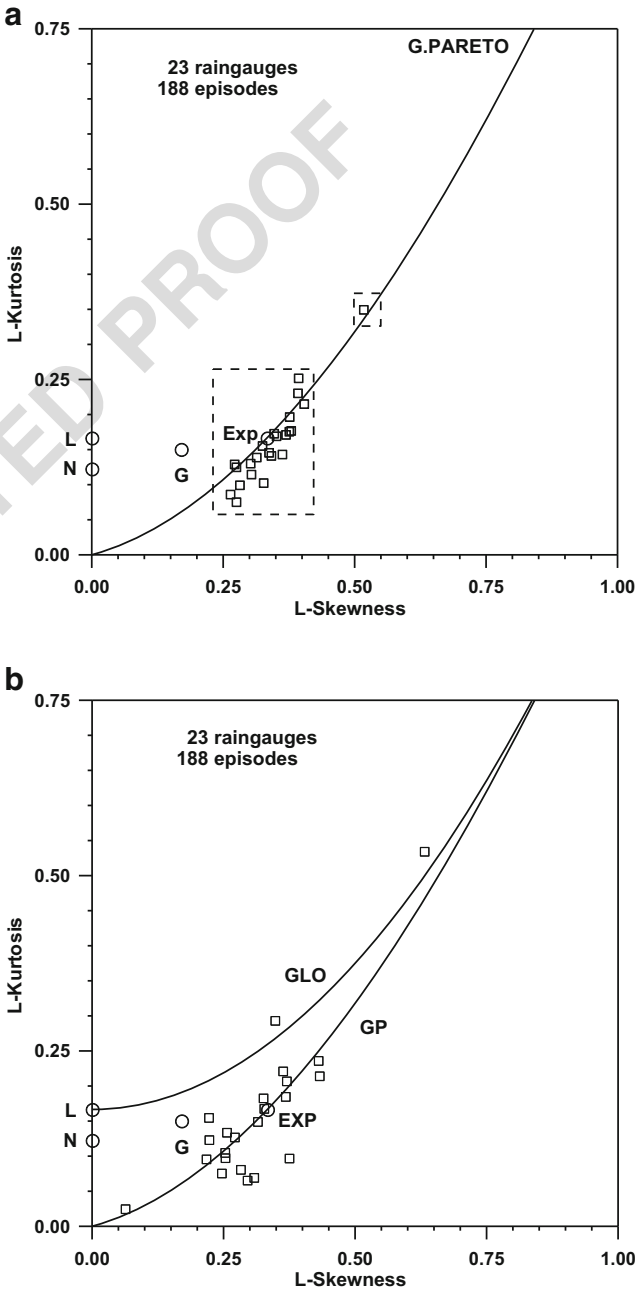

Fig. 2 L-skewness-kurtosis diagrams for statistical models and empiric τ_3 and τ_4 values for POT derived from **a** 95% percentile modelled as a GP distribution and from **b** the MEP modelled as GP and GLO distributions. Continuous lines represent GP or GLO distributions and EXP, G, N and L correspond to exponential, Gumbel, normal and logistic models

Scale, shape and location parameters now permit defining the range of validity of argument x, given by $\{-\infty \le x \le \delta + \alpha/\kappa\}$ if $\kappa > 0$, $\{-\infty \le x \le \infty\}$ if $\kappa = 0$ and $\{\delta + \alpha/\kappa \le x \le \infty\}$ if $k < 0$.

After selecting the best statistical model reproducing empiric distribution of extremes, the expected annual extreme for a certain return period T_r (in years) would be

$$T_r = 1/(1-F(x_r)) \tag{5}$$

being $F(x_r)$ the cumulative distribution function of $f(x_r)$ and x_r the value corresponding to a return period T_r. Bearing in mind that, in agreement with the POT method, samples of extremes are not chosen with a ratio of one per year, the return period derived from Eq. (5) would be given in units of 5-min episodes instead of years. Assuming that the number of extreme values is high enough, the substitution of T_r by $\beta \cdot T_r$ on Eq. (5), with β the average number of extreme values per year, permits interpreting x_r as the expected threshold to be exceeded for a return period given in years.

The expected return values x_r for the GP distribution, bearing in mind Eq. (5) and the average number of extreme values by year, β, can be expressed as

$$x_r = (\alpha/k)\left\{1-(\beta T_r)^{-k}\right\} + \delta \tag{6}$$

Similarly, the expected return values for the GLO distribution are given as

$$x_r = (\alpha/k)g(\beta T_r) + \delta \tag{7a}$$

with

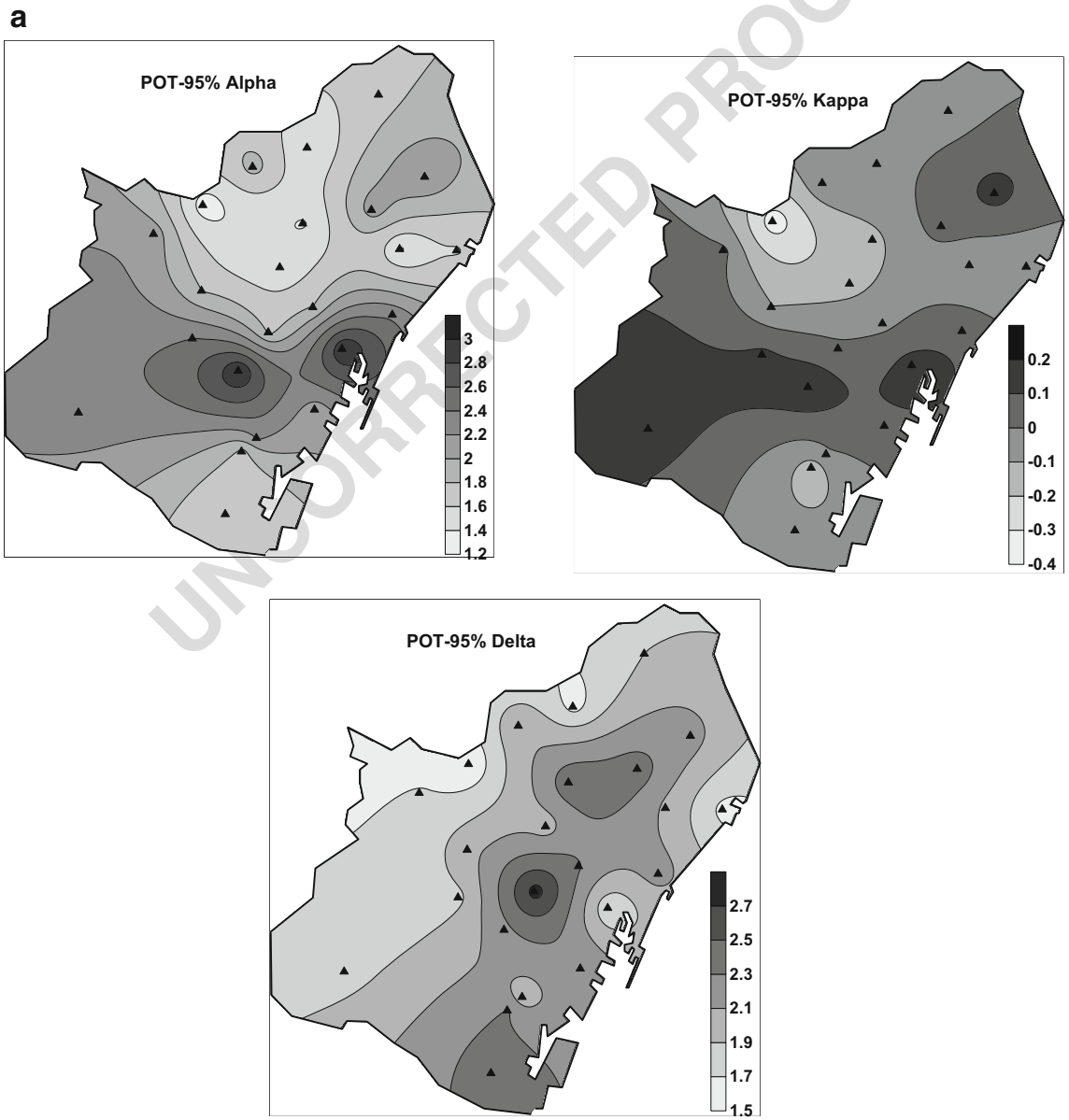

Fig. 3 Spatial distribution of parameters α, κ and δ of the GP distribution for POT derived from **a** 95% percentile and **b** the MEP

$$g(\beta T_r) = 1 - \frac{1}{(\beta T_r - 1)^k} \quad (7b)$$

The return values of the extreme 5-min amounts at the network gauges are both derived from the values above 95% percentile and from the MEP by applying Eqs. 6 and 7a and 7b.

Given that the analysed POT series are derived from wide samples (from 3520 to 4260 5-min amounts depending on the rain gauge), a high enough number of extreme intensities can be assured. Return period curves will be expanded up to 75 years. Nevertheless, taking into consideration the recording length of the urban rain rate network is 16 years, 5-min rain amounts for return periods longer than 25 years have to be carefully considered, as they have less reliability.

Finally, the AES are also obtained to make a complementary estimation of return values applying the generalised extreme value (GEV) distribution (Hosking and Wallis 1997). In agreement with Lana et al. (2006), the return period values are given as

$$x_r = (\alpha/k)[1 - g(T_r)] + \delta \quad (8a)$$

with

$$g(T_r) = \left\{ -ln\left(1 - \frac{1}{T_r}\right) \right\}^k \quad (8b)$$

α, κ and δ being the scale, shape and location parameters of the GEV distribution.

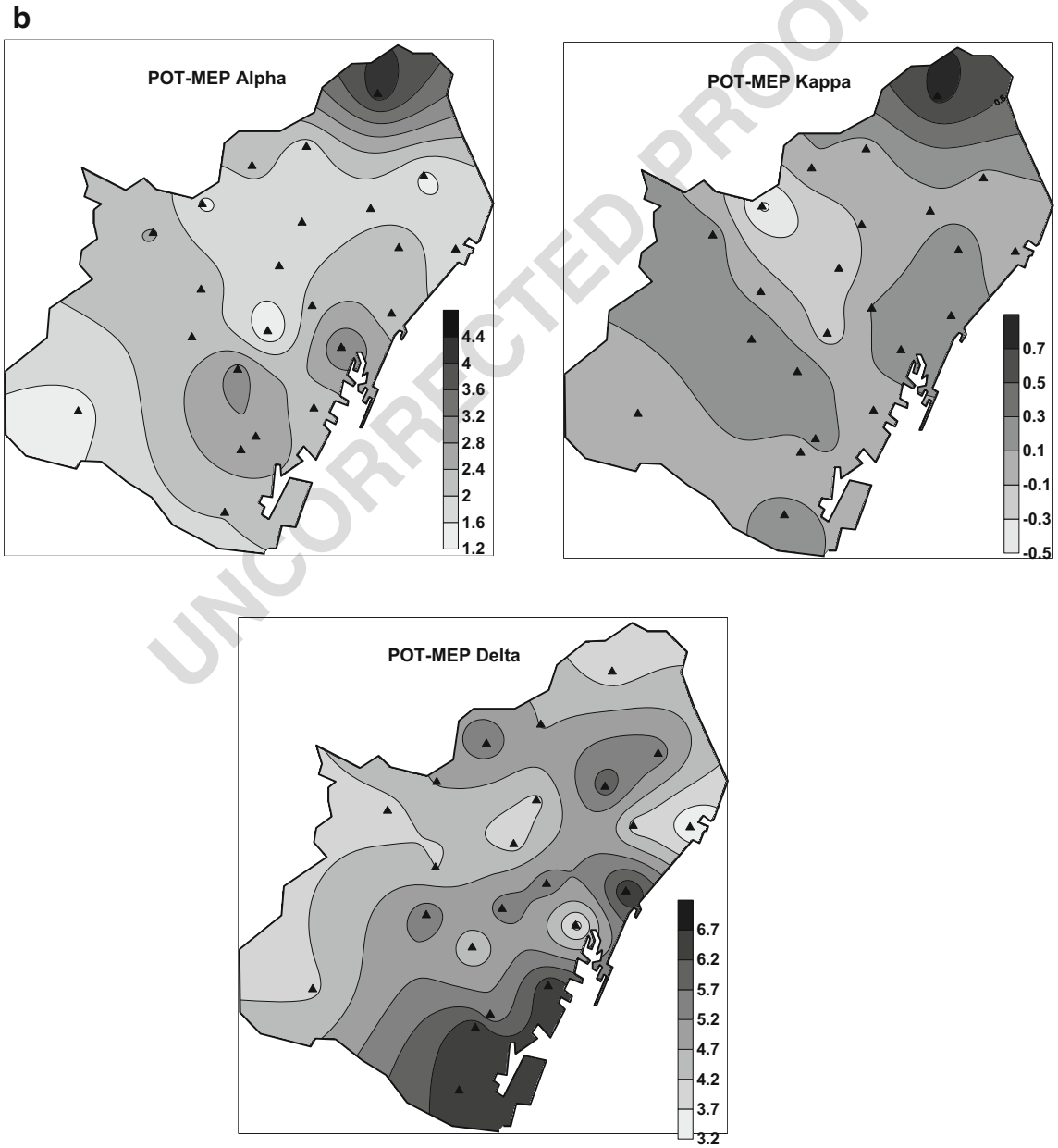

Fig. 3 (continued)

4 Results

4.1 Distribution function and sampling strategy

The best theoretical statistic model selection fitting the empiric distribution of extreme 5-min rain amounts is shown in Fig. 2a, b, where the L-skewness-kurtosis curves corresponding to GP or GLO models are compared with the respective empiric values. In agreement with these figures, it is quite evident that all 23 sets of rain intensities above the 95% percentile fit the GP model well. With respect to the MEP criterion, only two of these extreme series (gauges 3 and 10) would be better represented by the GLO instead of the GP model. Then, return period curves have been built for every gauge bearing in mind the respective best theoretical model.

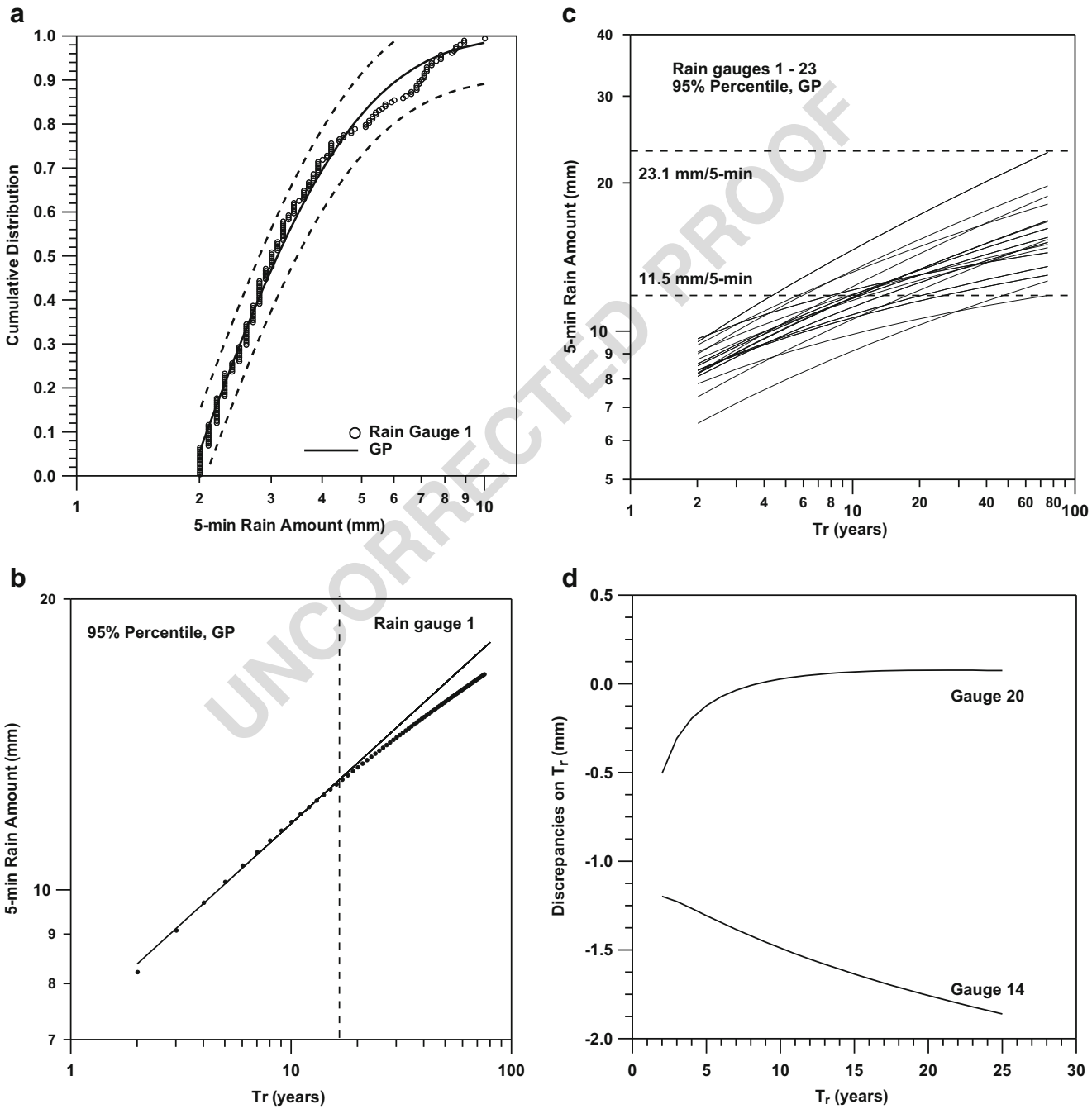

Fig. 4 **a** Fit of the POT by applying the 95% percentile to the GP distribution (gauge 1). Dashed lines correspond to the Kolmogorov-Smirnov 95% confidence bands and the thick continuous line represents the GP model. **b** Return period curves for the same gauge. **c** The 17 return period curves. **d** Maximum positive and negative discrepancies between return periods derived from 95% percentile with and without declustering

Figure 3a, b shows the spatial distribution of scale, shape and location parameters for 95% percentile and MEP strategies across Barcelona. As expected, location parameter δ gives a good description of the spatial variability of the thresholds defining POT. Additionally, scale and shape parameters also show different spatial patterns when comparing 95% percentile maps with MEP maps.

4.2 Return period curves

Figure 4a shows an example (gauge 1) of extreme 5-min amounts above the 95% percentile fitting the GP model well. Empirical extreme 5-min amounts are within 95% confidence bands of the Kolmogorov-Smirnov test (Benjamin and Cornell 1970; Press et al. 1992) quantified as $\pm 1.36/N^{1/2}$ taking into account that N represents a large enough number of data. The corresponding example of return period curve is shown in Fig. 4b, where a more smooth change on the increasing evolution of the return values for return periods approximately close to 15 years can be observed. The whole set of return period curves is shown in Fig. 4c, where the different behaviour of extreme 5-min amount curves becomes evident. First, whereas for $T_r = 2$ years extremes exceed a range approximately from 6.5 to 9.5 mm/5 min, for a return period of 75 years, this interval changes from 11.5 to 23.1 mm/5 min. And second, the smoothing of the return value increase (Fig. 4b) is also found for the other 16 rain gauges, being defined as a relatively wide range (10–20 years) for which the slope of return period curves begins to diminish. Consequently, in spite of the relatively small urban area (about 100 km^2), a different behaviour is found for every rain rate gauge, making the spatial heterogeneity of the extreme 5-min amounts on the urban area of Barcelona evident. Figure 4d shows two examples of the discrepancies on return periods between clustered and declustered 95% percentile series. While for gauge 14, the maximum discrepancies are detected (-1.8 mm/5 min) for 25 years, gauge 20 is characterised by almost null differences for return periods exceeding 5 years.

With respect to the MEP criterion, an example for gauge 10 is shown in Fig. 5. Whereas the evolutions of MEP for other climatic data, as dry spell lengths, are characterised by a linear evolution of MEP up to a critical threshold from which this linear trend disappears (Lana et al. 2006), extreme 5-min amounts depict a different behaviour. When exceeding the critical threshold, the initial linearity is substituted for a different linear evolution of MEP with a clear negative slope. Figure 6a–c schematises the process to obtain the return period curves from the GP distribution when applying the MEP criterion. Figure 6a shows the POT fitting the GP distribution for gauge 1 well as a common pattern for most of gauges, except for a few with a better fit to the GLO distribution. The return period curves also depict notable differences for the different gauges. As an example, Fig. 6b shows these curves for gauges 1 and 14, while Fig. 6c shows the whole set of curves for the 17 gauges considered. The behaviour of these curves becomes quite similar to that observed for POT selected according to 95% percentile criterion (Fig. 4c). Whereas the range of extreme values for $T_r = 2$ years is quite similar to that observed in Fig. 4c, the range (from 9.4 to 22.5 mm/5 min) is slightly different for $T_r =$ 75 years. Again, the spatial heterogeneity of the extreme 5-min amounts recorded at the urban network of Barcelona becomes quite evident.

The sets of POT derived from the MEP fitting GLO better instead of GP distribution stand only for a few gauges. The distribution for gauge 10 is shown in Fig. 7. In agreement with this figure, the fit of empiric POT to the GLO distribution is very good. The discrepancies on the extreme 5-min amounts, when comparing 95% percentile and MEP criteria for gauge 10, are small. Whereas for a return period of 2 years this discrepancy is almost null (0.2 mm/5 min), for 75 years, it achieves a modest value of 2.5 mm/5 min.

Table 2 shows the return period values for 2, 5, 10 and 25 years applying AES and POT (95% percentile, with and without declustering process, and MEP) strategies. While for 2, 5 and 10 years the absolute discrepancies between expected intensities depending on the sampling strategy are kept below 2.0 mm/5 min, for 25 years, these discrepancies are almost null except for

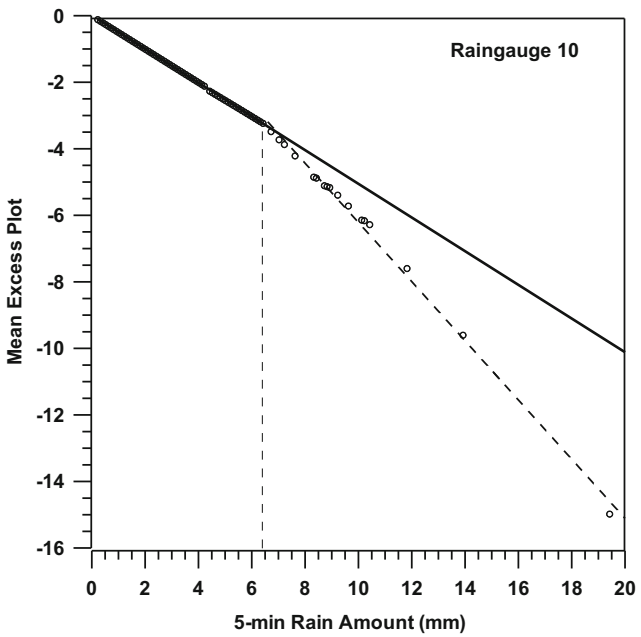

Fig. 5 MEP criterion applied to gauge 10

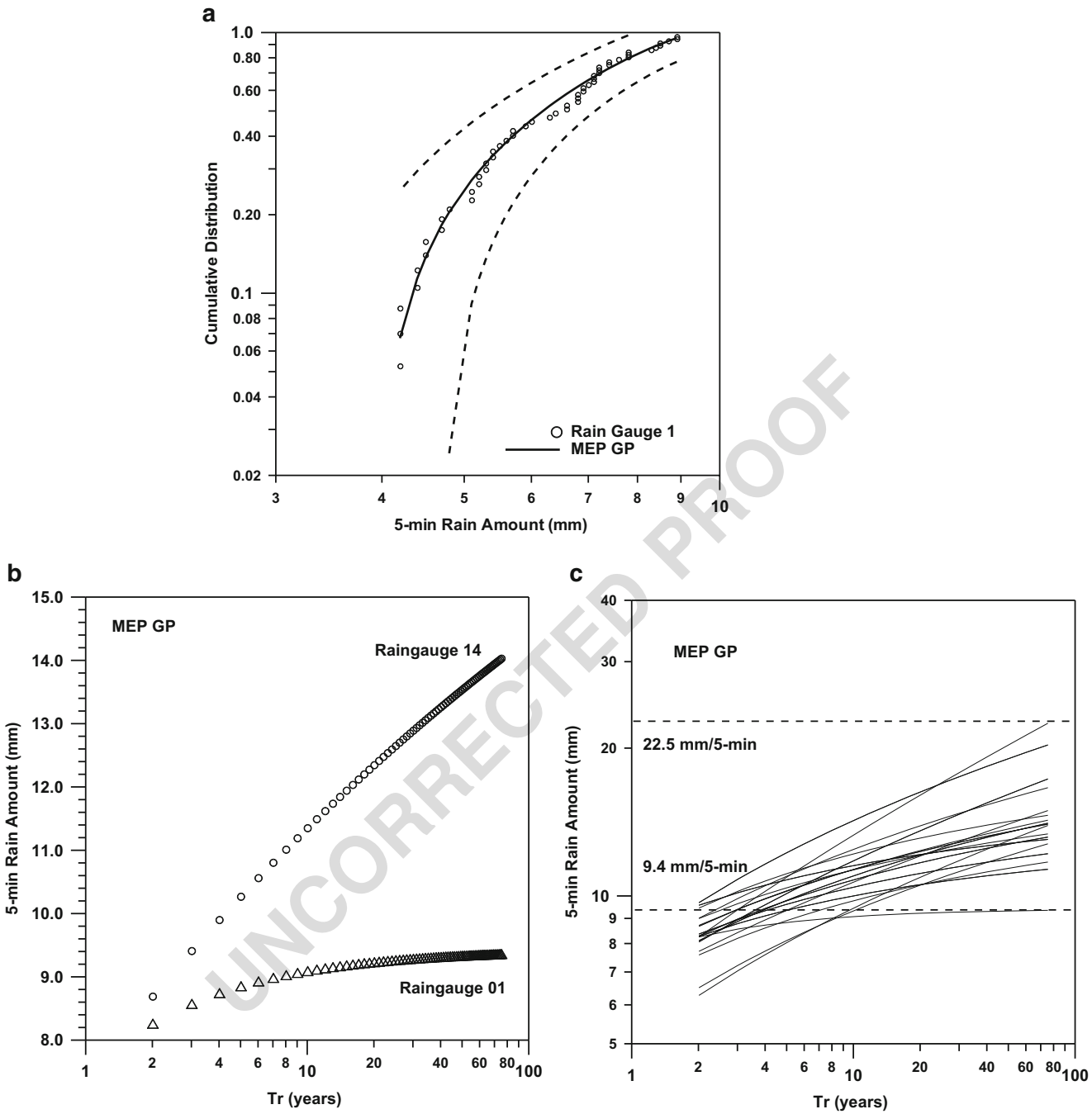

Fig. 6 **a** Fit of the POT by applying the MEP to the GP distribution (gauge 1). Dashed lines are the Kolmogorov-Smirnov 95% confidence bands and the thick continuous line represents the GP distribution. **b** Return period curves for gauges 1 and 14. **c** The 17 return period curves

gauge number 2. The largest absolute difference for this gauge (4.6 mm/5 min for 25 years) is found when comparing AES and POT (95% percentile) strategies. When considering declustered series derived from 95% percentile, 12 out of 17 return period curves depict slightly lesser 5-min rain amounts than those derived without declustering. Average discrepancies for the 2–25-year range vary from 0.1 to 1.5 mm/5 min with standard deviations from 0.1 to 1.3 mm/5 min. For only five rain gauges, their discrepancies on average return period values are of opposite sign to the previous case, being slightly increased than those corresponding to the declustered series instead of those not declustered. In these cases, the average discrepancy varies from 0.1 to 0.64 mm/5 min and the standard deviation from 0.14 to 0.75 mm/5 min.

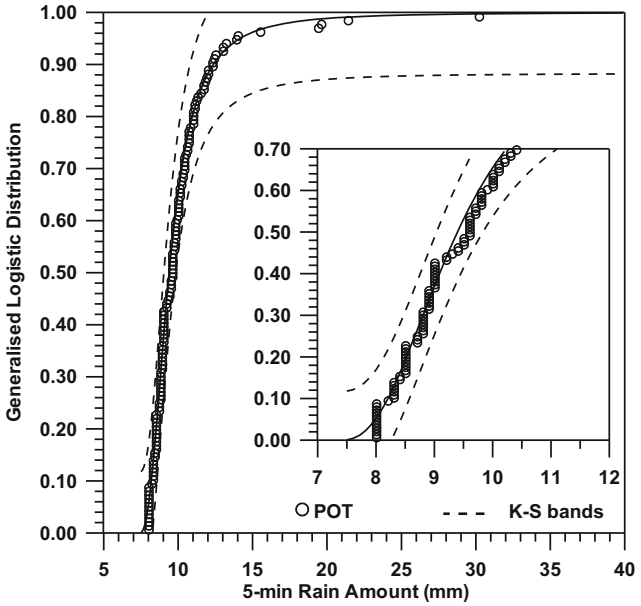

Fig. 7 Fit of the POT by applying the MEP to the GLO distribution (gauge10). Dashed lines are the Kolmogorov-Smirnov 95% confidence bands and the thick continuous line represents the GLO distribution

Table 3 summarises the respective thresholds for the 95% percentile and MEP strategies. Systematically, thresholds derived from MEP (from 3.0 up to 6.8 mm/5 min) are higher than those obtained applying 95% percentile (from 1.5 to 2.9 mm/5 min), being their absolute difference below 2.5 mm/5 min, except for gauges 18 and 20 with discrepancies above 4.0 mm/5 min. As percentiles associated with MEP thresholds keep systematically above 95%, MEP criterion is more restrictive than 95% percentile when defining POT to obtain return period curves. It is worth mentioning that discrepancies between 95% percentile and those obtained from MEP (in some cases close to 99% percentile) are a bit larger in comparison with, for instance, analysis of extreme dry spell lengths (Lana et al. 2006). In spite of these high thresholds, the number of 5-min amounts is high enough to build POT series leading to confident results, provided that the declustering process is not applied to the MEP series.

4.3 Overall linear time trends

Another relevant question is the possibility of time trends on POT series. If these trends were notably high, return period curves, based on stationary POT, could be submitted to some biases leading to over-/underestimation of predicted extreme 5-min amounts. Figure 8 shows the time evolution of extreme 5-min amounts above 6.0 mm/5 min, the threshold to be exceeded by rainfall intensities with a return period of 2 years. It can be assessed that the small negative global linear trend of −0.11 mm/5 min/year is characterised by a Mann-Kendall statistic (Mitchell et al. 1966) of −0.07. In short, this possible small time trend is not statistically significant, given that its confidence level would be less than 5%. Consequently, it can be assumed that extreme 5-min rain amounts along the recording period would be only submitted to fluctuations and then return period curves should be accepted. It should be also considered that the number of empiric extremes shown in Fig. 8 is small but not negligible (60 values), permitting a right

Q5 **Table 2** Extreme 5-min rain amounts (mm/5 min) obtained with the AES, 95% percentile and the MEP criteria for return periods from 2 to 25 years for the selected 17 gauges

Gauge	$T_r = 2$ years				$T_r = 5$ years				$T_r = 10$ years				$T_r = 25$ years			
	AES	95%	95%*	MEP	AES	95%	95%*	MEP	AES	95%	95%*	MEP	AES	95%	95%*	MEP
1	7.2	8.2	7.4	8.3	8.7	10.2	9.3	8.9	9.4	11.8	10.7	9.1	10.2	14.0	12.4	9.3
2	7.5	7.8	7.1	7.7	10.1	9.1	8.9	9.4	12.2	9.9	10.2	10.7	15.5	10.9	11.9	12.6
5	7.1	9.0	7.2	9.0	10.0	11.4	9.8	11.0	12.0	13.3	12.1	12.5	15.0	16.1	15.4	14.4
6	7.0	8.2	6.5	8.3	9.7	10.5	9.1	11.0	12.0	12.4	11.2	13.3	15.7	15.1	14.3	17.1
7	8.2	9.4	8.3	9.5	10.7	11.6	10.8	11.1	12.2	13.2	12.7	12.2	14.0	15.4	15.0	13.4
8	6.4	6.5	5.7	6.5	8.4	8.0	7.3	8.1	9.7	9.1	8.5	9.4	11.4	10.7	10.0	10.9
9	6.4	7.4	6.5	7.6	8.4	9.2	8.3	8.9	9.6	10.6	9.7	9.8	11.0	12.7	11.6	10.8
10	8.3	9.5	8.4	9.7	11.9	12.3	11.5	12.3	14.6	14.7	14.1	14.3	18.3	18.2	18.0	17.0
11	7.7	9.7	8.5	9.6	10.0	11.2	11.2	10.8	11.7	12.2	12.6	11.6	14.0	13.3	14.8	12.4
14	7.2	8.6	7.4	8.7	9.4	10.5	9.2	10.3	10.9	11.9	10.4	11.4	13.0	13.8	12.0	12.7
15	7.9	8.2	7.4	8.3	10.0	10.2	9.3	9.8	11.4	11.7	10.7	10.8	13.1	13.9	12.6	12.0
16	7.5	8.3	7.5	8.3	8.9	9.7	9.4	9.4	9.9	10.7	10.9	10.0	11.3	11.8	12.6	10.7
17	7.7	8.1	7.0	8.1	10.0	9.9	9.1	9.8	11.2	11.2	10.7	11.0	12.5	13.0	12.7	12.5
18	7.1	8.4	7.6	8.1	9.4	9.8	9.7	10.1	11.2	10.8	11.2	11.8	13.7	12.1	13.0	14.2
19	7.5	8.5	6.8	8.4	9.8	10.3	9.4	9.6	11.0	11.7	11.5	10.4	12.2	13.5	14.5	11.3
20	8.6	9.1	8.6	9.0	10.6	10.7	10.6	10.4	11.6	11.9	11.9	11.3	12.7	13.4	13.5	12.4
22	7.7	8.8	7.5	8.7	9.6	10.4	9.7	10.3	10.8	11.6	11.4	11.4	12.1	13.1	13.7	12.7

*Results obtained for declustered series are designed as 95%

JnlID 704_ArtID 2434_Proof# 1 - 01/03/2018

t3.1 **Table 3** Five-minute rain amount thresholds, given in mm/5 min, to select POT from 95% percentile and MEP. Corresponding percentiles for the MEP option are also included

t3.2	Gauge	95% percentile (mm/5 min)	MEP (mm/5 min)	MEP (%)
t3.3	1	2.0	4.2	98.7
t3.4	2	1.9	4.2	98.2
t3.5	3	1.5	3.8	99.1
t3.6	4	2.4	4.0	98.5
t3.7	5	2.1	4.2	98.4
t3.8	6	2.0	4.2	98.8
t3.9	7	2.1	4.2	98.9
t3.10	8	1.7	4.8	99.5
t3.11	9	2.0	4.2	98.8
t3.12	10	2.4	6.1	99.4
t3.13	11	2.4	4.2	97.6
t3.14	12	2.9	4.2	98.9
t3.15	13	1.7	3.0	98.0
t3.16	14	2.3	4.2	99.1
t3.17	15	2.4	4.0	99.5
t3.18	16	2.0	4.2	99.1
t3.19	17	2.2	4.2	99.2
t3.20	18	2.4	6.6	99.6
t3.21	19	1.9	4.2	98.3
t3.22	20	2.3	6.8	99.4
t3.23	21	2.2	5.4	99.0
t3.24	22	2.5	6.0	99.1
t3.25	23	1.9	3.4	97.3

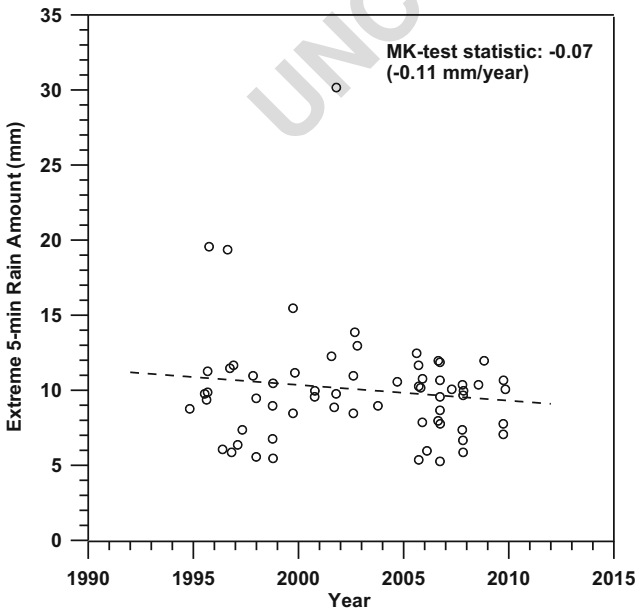

Fig. 8 Global linear time trend for extreme 5-min amounts exceeding theoretical values derived for 2 years return period

Mann-Kendall statistic quantification. Nevertheless, a sampling length of 16 years does not allow a confident extrapolation of this global time trend.

4.4 Spatial distribution of extreme 5-min rain amounts

The spatial distributions of extreme 5-min amounts for return periods of 10, 25 and 50 years are shown in Fig. 9a, b. It is worth mentioning the spatial heterogeneity of the expected intensity, with two nuclei of maximum extreme intensity (gauges 6 and 10) close to the Barcelona harbour and the Littoral chain. The spatial distribution of the return period maps may be strongly influenced by the topography of the city and neighbouring areas. For example, when eastern and south-eastern advections provide heavy rains, the nucleus of maximum extremes close to the Barcelona harbour is windward of a low hill (150 m a.s.l.), with a strong steep slope facing the coast (Fig. 1). The other nucleus of maximum extremes appears very close to the Littoral chain (500 m a.s.l.). Very likely, the same causes concerning eastern advections proposed for the first nucleus would be right for the second. With respect to areas with the lowest extremes, one of these is detected along the seaside. The other appears towards the western limit of Barcelona City, close to the lowest heights of the Littoral chain and the plain southern of the urban area. In short, the spatial variability of extreme 5-min amount regime is clearly shown in Figs. 3a, b and 9a, b.

5 Conclusions

It has been verified that most of the 23 time series of extreme 5-min rain amounts fit very well the GP distribution, whatever the criterion considered (95% percentile or MEP) to select the POT. Only for two gauges is the best fit obtained by using the GLO distribution for MEP methodology. With respect to the return period curves, some differences have been found between predicted extremes based on 95% percentile and MEP criteria. Nevertheless, except for a small number of gauges, these discrepancies are not very relevant, especially for medium and short return periods. Additionally, absolute discrepancies between AES and POT strategies are small, except for gauge number 2 and return periods of 25 and 50 years, for which these discrepancies achieve a maximum of 7.0 mm/5 min. Given that the number of recording years is low for a confident estimation of AES, return period curves derived from POT should be more confident. Even though the thresholds for 95% percentile differ from those derived from the MEP strategy (Table 3), it is worth mentioning that return period maps for 5, 10 and 25 years (Fig. 9a, b) from both strategies show very similar geographic patterns and 5-min amounts. Also, the differences between return period values

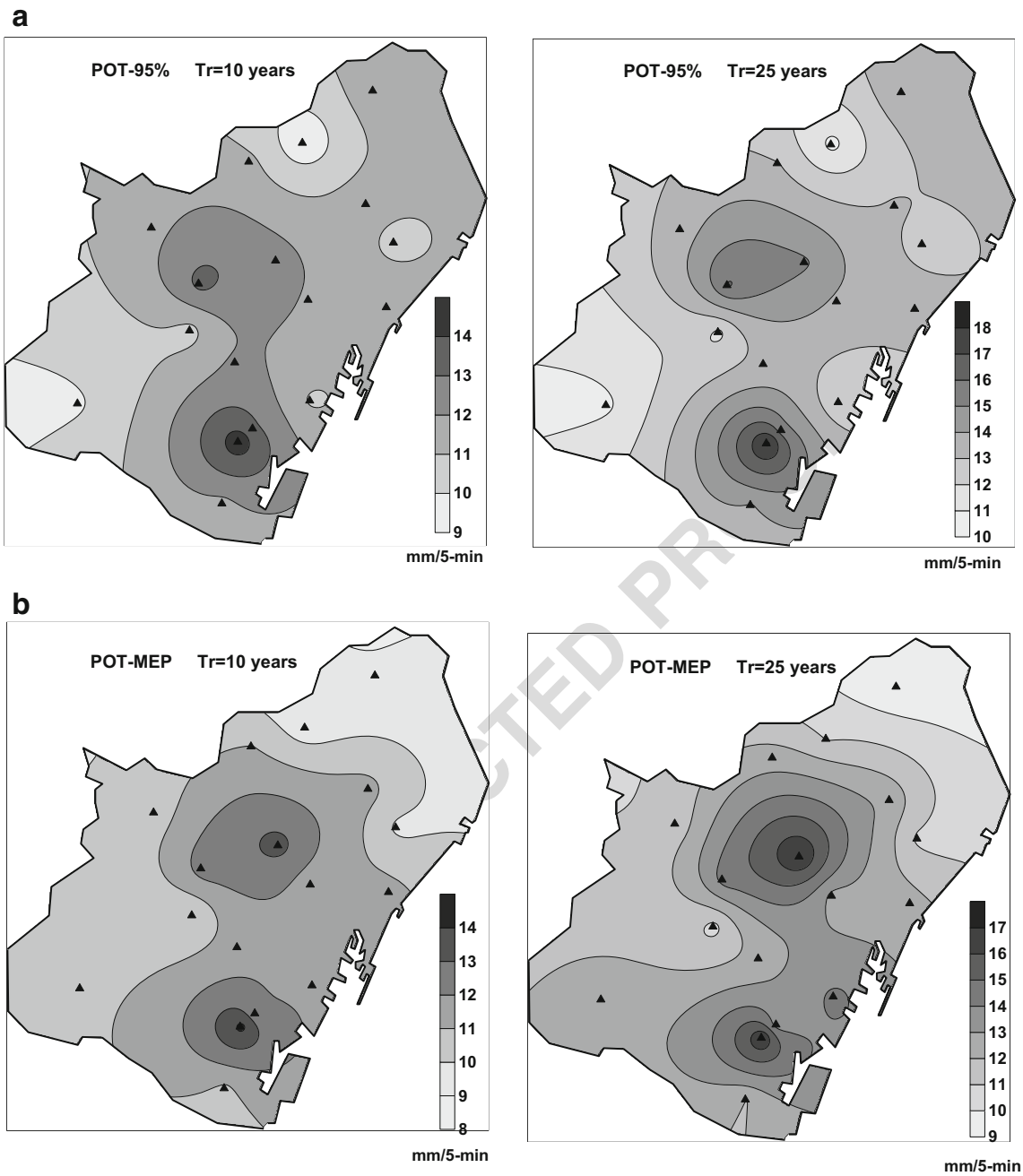

Fig. 9 Return period maps (10 and 25 years) covering the urban area of Barcelona for POT obtained by applying **a** 95% percentile and **b** the MEP. Rain rates are given in mm/5 min

derived from 95% percentile with and without declustering process suggest that the discrepancies are not very relevant in most cases. In consequence, two questions should be considered before deducing practical consequences derived from the declustering process. On one hand, the independence of extremes should be guaranteed and the mathematical theory of statistical extreme distribution rightly applied. On the other hand, the risk of flash floods would be only partially considered due to the declustering process, given that relevant 5-min rain amounts close to a declustered extreme would not be considered.

From an applied point of view, it is relevant that the detection of maximum extremes for the three return period maps of 5, 10 and 25 years (Fig. 9) can be interpreted and justified in terms of topographic patterns of Barcelona City and neighbouring areas, as also in terms of atmospheric dynamics, as convective processes and eastern and south-eastern advections, which also notably contribute to rain amounts at monthly and annual scales. The short recording period of the Barcelona network (years 1994–2009) could be a shortcoming to derive confident return period maps for long return periods. Nevertheless, relatively short periods (below 25 years) could

be used to quantify flood risks and improve drainage systems. For instance, for a return period of just 10 years, a great percentage of the urban area could be affected by extreme intensities exceeding 11–12 mm/5 min, which would increase above 13–14 mm/5 min according to the return period map of 25 years. Finally, it has to be remembered that the global linear time trend on extreme records is negative, small and not statistically significant. In consequence, it cannot be considered as a factor biasing predicted extreme 5-min amounts. Consequently, Barcelona flood risks in the near future would be inherent to the statistics of the return period curves, but not due to remarkable changes on atmospheric dynamics notably increasing or decreasing the intensity of 5-min episodes. In short, the present analysis should contribute to improving the knowledge on urban flood risks and to designing better drainage strategies to mitigate the effects of very heavy rainfalls.

Appendix. Kendall-τ test of independence

If a set of $\{z_i\}$, $i = 1,\ldots,n$, peaks are selected from a time series and their associated ranks, $\{R_i\}$ are determined, the Kendall-τ test can be applied to verify the independence of the series, usually with a probability exceeding 95%. After obtaining the set of rank pairs $\{(R_1, R_2), (R_2, R_3), \ldots..., (R_{n-1}, R_n)\}$, the number of discordances n_d or, in other words, the number of pairs (R_i, R_{i+1}) and (R_j, R_{j+1}) accomplishing either $R_i < R_j$ and $R_{i+1} > R_{j+1}$ or $R_i > R_j$ and $R_{i+1} < R_{j+1}$, with $i = 1,\ldots,n-1$, $j = 1,\ldots,n-1$ and $i \neq j$ leads to the empiric Kendall-τ statistic

$$\tau_{\text{emp}} = 1 - \frac{4n_d}{(n-1)(n-2)} \tag{9}$$

The null hypothesis of independent $\{z_i\}$ peaks approaches τ to a normal random variable, provided that the number of samples n exceeds 10. The expected value of τ will be

$$<\tau> = -\frac{2}{3(n-1)} \tag{10}$$

and its variance

$$\sigma^2(\tau) = \frac{20n^3 - 74n^2 + 54n + 148}{45(n-1)^2(n-2)^2} \tag{11}$$

If τ_{emp}, given by Eq. (9), does not exceed

$$\tau_{0.95} = <\tau> + 1.65\sigma(\tau) \tag{12}$$

the one-sided 95% test permits accepting the null hypothesis of $\{z_i\}$ independence with 95% confidence.

References

Acero FJ, García JA, Gallego MC (2011) Peaks-over-threshold study of trends in extreme rainfall over the Iberian Peninsula. J Clim 24: 1089–1105

Alhakim A, Hooper W (2008) A non-parametric test for several independent samples. Journal of Nonparametric Statistics 20(3):253–261. https://doi.org/10.1080/10485250801976741

Anagnostopoulou C, Tolika K (2012) Extreme precipitation in Europe: statistical threshold selection based on climatological criteria. Theor Appl Climatol 107:479–489

Beguería S (2005) Uncertainties in partial duration series modelling of extremes related to the choice of the threshold value. J Hydrol 303: 215–230

Beguería S, Vicente-Serrano SM, López-Moreno JI, García-Ruíz JM (2009) Annual and seasonal mapping of peak intensity, magnitude and duration of extreme precipitation events across a climatic gradient, North-East Spain. Int J Climatol 29:1759–1779

Beguería S, Angulo-Martínez M, Vicente-Serrano SM, López-Moreno JI, El-Kenawi A (2011) Assessing trends in extreme precipitation events intensity and magnitude using non-stationary peaks-over-threshold analysis: a case study in North-East Spain from 1930 to 2006. Int J Climatol 31:2102–2114

Benjamin JR, Cornell CA (1970) Probability, statistics and decision for civil engineers. McGraw-Hill Inc., New York NY

Burgueño A, Serra C, Lana X (2004) Monthly and annual statistical distributions of the daily rainfall at the Fabra Observatory (Barcelona, NE Spain) for the years 1917–1999. Theor Appl Climatol 77:57–75

Casas MC, Codina B, Redaño A, Lorente J (2004) A methodology to classify extreme rainfall events in the western Mediterranean area. Theor Appl Climatol 77:139–150. https://doi.org/10.1007/s00704-003-0003-x

Casas MC, Rodríguez R, Redaño A (2010) Analysis of extreme rainfall in Barcelona using a microscale rain gauge network. Meteorol Appl 17:117–123. https://doi.org/10.1002/met.166 http://hdl.handle.net/2117/6733

Chen YR, Chu P-S (2014) Trends in precipitation extremes and return levels in the Hawaiian Islands and their changing climate. Int J Climatol 34:3913–3925

Claps P, Laio F (2003) Can continuous streamflow data support flood frequency analysis? An alternative to the partial duration series approach. Water Resour Res 39:1216

Coles S (2001) An introduction to statistical modeling of extreme values. Springer Science and Business Media, 208 pp

Ferguson TS, Genest C, Hallin M (2000) Kendall's tau for serial dependence. Canadian Journal of Statistics 28:587–604

Hosking JRM, Wallis JR, Wood EF (1985) Estimation of the generalised extreme value distributions by the method of probability-weighted moments. Techtonometrics 27:251–261

Hosking JRM, Wallis JR (1997) Regional frequency analysis. Cambridge University Press, Cambridge, 224 pp

Kendall MG, Stuart A (1967) The advanced theory of statistics, vol 2. Inference and relationship, 2nd edn. Griffin, London

Kysely J, Picek J, Veranová R (2010) Estimating extremes in climate change simulations using the peaks-over-threshold method with non-stationary threshold. Glob Planet Chang 72:55–68

Lana X, Burgueño A, Martínez MD, Serra C (2006) Statistical distributions and sampling strategies for the analysis of extreme dry spells in Catalonia (NE Spain). J Hydrol 324:94–114

Lana X, Martínez MD, Serra C, Burgueño A (2005) Periodicities and irregularities of indices describing the daily pluviometric regime of the Fabra Observatory (NE Spain) for the years 1917–1999. Theor Appl Climatol 82:183–198

Lana X, Serra C, Casas-Castillo MC, Rodríguez-Solà R, Redaño A, Burgueño A (2017) Rainfall intensity patterns derived for the urban network of Barcelona (NE Spain). Theor Appl Climatol. https://doi.org/10.1007/s00704-017-2193-7

Lorente J, Redaño A (1990) Rainfall rate distribution in a local scale: the case of Barcelona City. Theor Appl Climatol 41:23–32

Mitchell JM, Dzerdzeevskii B, Flohn H, Hofmeyr WL, Lamb HH, Rao KN, Wall'en CC. 1966. Climatic change. Technical Note, No. 79. World Meteorological Organization: Geneva, Switzerland, 99

Press WH, Teukolsky SA, Vetterling WT, Flannery BP (1992) Numerical recipes in C. The art of scientific computing. Cambridge University Press, Cambridge, 994 pp

Rodríguez, R., Navarro, X., Casas, M.C., Redaño, A. (2013a). Rainfall spatial organization and areal reduction factors in the metropolitan area of Barcelona (Spain). Theor Appl Climatol, 114, 1–8. DOI: https://doi.org/10.1007/s00704-012-0818-4. http://hdl.handle.net/2117/17169

Rodríguez, R., Casas, M.C., Redaño, A. (2013b). Multifractal analysis of the rainfall time distribution on the metropolitan area of Barcelona (Spain). Meteorol Atmospheric Physics, 121(3–4): 181–187, doi https://doi.org/10.1007/s00703-013-0256-6. http://hdl.handle.net/2117/19110

Rodríguez-Solà R, Casas-Castillo MC, Navarro X, Redaño A (2016) A study of the scaling properties of rainfall in Spain and its appropriateness to generate intensity-duration-frequency curves from daily records. Int J Climatol 37:770–780. https://doi.org/10.1002/joc.4738. http://hdl.handle.net/2117/87312

Sneyers R (1990) On the statistical analysis of series of observations. In: Technical note 415. WMO, Geneva

Vicente-Serrano SM, Beguería-Portugués S (2003) Estimating extreme dry-spell risk in the middle Ebro valley (NE Spain): a comparative analysis of partial duration series with general Pareto distribution and annual maxima series with a Gumbel distribution. Int J Climatol 23:1103–1118

Villarini G, Smith JA, Ntelekos AA, Schwartz U (2011) Annual maximum and peaks-over-threshold analyses of daily rainfall accumulations for Austria. J Geophys Res 116:D05103